

Pressure-induced breakdown of a correlated system: The progressive collapse of the Mott-Hubbard state in $R\text{FeO}_3$

W. M. Xu,¹ O. Naaman,¹ G. Kh. Rozenberg,¹ M. P. Pasternak,^{1,2} and R. D. Taylor²

¹*School of Physics and Astronomy, Tel Aviv University, 69978 Tel Aviv, Israel*

²*MST-10, MS-K764, Los Alamos National Laboratory, Los Alamos, New Mexico 87545*

(Received 21 February 2001; published 7 August 2001)

Mössbauer spectroscopy, resistance, and synchrotron x-ray-diffraction (XRD) methods were combined for detailed studies of the pressure-induced breakdown of the strongly correlated perovskite $R\text{Fe}^{3+}\text{O}_3$ ($R = \text{La, Pr}$) systems. The XRD studies have shown that in the range 30–50 GPa both orthorhombic perovskites undergo a first-order phase transition to a new high-pressure (HP) phase accompanied by a $\sim 3\%$ volume contraction. The HP phases at $P < 50$ GPa are characterized by the coexistence, with equal abundance, of high ($S = \frac{5}{2}$, ${}^6A_{1g}$) and low-spin ($S = \frac{1}{2}$, ${}^2T_{2g}$) Fe^{3+} sublattices. With further pressure increase a gradual high- to low-spin transition occurs, fully converting to an $S = \frac{1}{2}$ state at ~ 65 GPa for both La and Pr. For PrFeO_3 up to 90 GPa, the highest pressure reached with MS in this compound, and for LaFeO_3 between 70–120 GPa, magnetic spin-spin relaxation spectra are observed suggesting the presence of a weak magnetic exchange. This coincides with a drastic decrease in the resistance. The observation of spin-lattice paramagnetic relaxation in spectra in the 120- to 170-GPa range for LaFeO_3 concurs with the onset of a metallic state with noninteracting moments as evidenced by $R(P, T)$ studies. It is predicted that a normal metal, with no moments, will be established in LaFeO_3 at ~ 240 GPa. A detailed analysis of the magnetic interactions in an antiferromagnetic insulator at very high pressures and a Mott-Hubbard phase diagram are presented in terms of the pressure versus the magnetic moment.

DOI: 10.1103/PhysRevB.64.094411

PACS number(s): 62.50.+p, 61.10.-i, 71.30.+h, 76.80.+y

I. INTRODUCTION

The majority of transition-metal (TM) compounds are systems with strongly correlated electrons, the so-called Mott insulators.¹ These compounds, characterized by large optical gaps and large on-site magnetic moments determined by Hund's rules, may undergo an insulator-metal transition (IMT) either by the filling of carriers due to chemical doping or by high external pressure.² Whereas the first process will affect the U/t ratio by decreasing the value of the Coulomb repulsion energy U ,³ the aftermath of the second process will be an increase of the d -band width W and therefore of the kinetic energy t . In principle both methods can provide variations in U/t for the investigation of the Mott-Hubbard system phase diagram. However, the main problem with chemical doping is that intricate and uncontrollable interactions may occur in such narrow d -band systems resulting in an undesired electronic and structural disorder and other complex phenomena unrelated to the Mott-Hubbard phenomenon.⁴ Thus, external static pressure is the cleanest, most preferable way to study the phase diagram of a Mott insulator in terms of U/t only.

Previous high-pressure (HP) studies with NiI_2 (Ref. 5) and other TM halides⁶ revealed the phenomenon of an abrupt correlation breakdown (Mott transition) manifested by an IMT concurrent with the collapse of the TM ion's magnetic moments. Recent HP studies in Fe_2O_3 (Ref. 7) demonstrated the occurrence of a Mott transition (gap closure) that resulted in or was the cause of a first-order phase transition resulting in a 10% volume decrease at ~ 70 GPa. In all those cases the abruptness of the transition with pressure, from a $U/t > 1$ to $U/t < 1$ regime, did not allow for

comprehensive examination of the Mott-Hubbard state in the intermediate $U/t \sim 1$ range. In this paper we present detailed experimental studies of a progressive breakdown of a strongly correlated system using the rare-earth orthoferrites $R\text{FeO}_3$ ($R = \text{La, Pr}$), a typical case of wide-gap, high-spin ($S = \frac{5}{2}$) Mott insulators. This was accomplished by carefully monitoring the pressure-induced evolution of the system structure, its magnetic moments and their interactions, and its electrical transport properties. It will be shown how complex and yet intimate the relationship is between the electric and magnetic properties within an isotherm as one progresses from a highly correlated regime ($U/t \gg 1$) through the twilight zone of the insulator-metal transition ($U/t \leq 1$) into a correlated metal, and culminating in a normal-metallic state ($U/t \ll 1$). Studies were carried out using the combined methods of synchrotron x-ray diffraction (XRD), electrical resistance [$R(P, T)$], and ${}^{57}\text{Fe}$ Mössbauer spectroscopy (MS) in conjunction with diamond-anvil cells at static pressures to ~ 200 GPa.

II. EXPERIMENT

The $R\text{FeO}_3$ were synthesized by a solid-solid reaction in air of stoichiometric amounts of spectroscopical pure $R_2\text{O}_3$ and Fe_2O_3 (enriched to 25% ${}^{57}\text{Fe}$) at 1200 °C. The composition and magnetic properties of the samples at ambient pressure were confirmed by conventional powder XRD and MS. The Tel-Aviv University miniature piston/cylinder⁸ diamond anvil cell (DAC) was used with anvils having $\sim 200\text{-}\mu\text{m}$ diameter culet size. Samples were encapsulated in 100- μm cavities drilled in stainless-steel gaskets for XRD and resistivity measurements and in a Re gasket for MS studies. Re also served as a collimator for the 14.4-keV γ rays. For the

XRD and MS studies Ar was used as a pressurizing medium.⁹ Ruby fluorescence served as a manometer.

X-ray-diffraction measurements with synchrotron radiation were carried out at 300 K in the angle dispersive mode using the monochromatic beam of the ID 30 station at the European Synchrotron Radiation Facilities (ESRF) and in the energy dispersive mode at the Cornell High Energy Synchrotron Source (CHESS) B-1 station. At ESRF the diffraction images were collected at a $\lambda = 0.4246 \text{ \AA}$ wavelength using image plates with typical exposure times of 5 min. Data were analyzed using the FIT2D program.¹⁰ At CHESS a Ge detector was employed. The diffraction patterns were analyzed using the DATLAB fitting program.¹¹

Resistance studies in the 4- to 300-K range were performed with miniature Pt electrodes insulated from the metal gasket by a mixture of alumina and NaCl. The DAC was mounted in a special holder device inserted into a commercial liquid-He Dewar. Using a PC-controlled dc motor-drive system, the DAC was gradually lowered and cooled by the cold He gas while recording simultaneously the temperature from a calibrated Si-diode thermometer and the resistance using the four-probe method.

Mössbauer studies were carried out with a $^{57}\text{Co}(\text{Rh})$ 10-mCi point source in the 4–300 K temperature range using a top-loading liquid-He cryostat.¹² Typical collection time of a single spectrum was ~ 24 h. All spectra were analyzed using appropriate fitting programs from which the hyperfine interaction parameters and the corresponding relative abundances of spectral components were derived. In the present studies, after previous studies with LaFeO_3 to 60 GPa,¹³ emphasis was given to PrFeO_3 in the 0–90 GPa and to LaFeO_3 in the 50- to 170-GPa regimes.

III. RESULTS

A. The phase transition and the coexistence zone

At ambient pressure and low pressure (LP) the $R\text{FeO}_3$ perovskites crystallize in the $Pbnm$ space group, a distorted orthorhombic structure derivative of cubic perovskites. The room-temperature $V(P)$ dependencies of LaFeO_3 and PrFeO_3 are shown in Figs. 1 and 2, respectively. Both orthoferrites undergo a sluggish structural phase transition; the HP phase is first detected at ~ 35 GPa, and the transition is fully completed by ~ 50 GPa. Within this pressure range both HP and LP coexist. Diffraction patterns of the PrFeO_3 HP phase could be tentatively attributed to the same orthorhombic perovskite structure but with a reduced c axis; for LaFeO_3 the structural transition near 30 GPa could be attributed to the transition to a tetragonal phase. Detailed HP-XRD analyses of several $R\text{FeO}_3$ ($R = \text{La}, \text{Pr}, \text{Eu}, \text{Y}, \text{and Lu}$) orthoferrites will be published.

Evidence that the volume shrinkage affects the Fe-O distances also can be deduced from the isomer shift (IS) measured by the Mössbauer effect. Within the LP regime the IS [which for ^{57}Fe is proportional to the negative value of the s -electron density $\rho_s(0)$ at the Fe nucleus] decreases progressively due to the volume decrease. However, at the phase

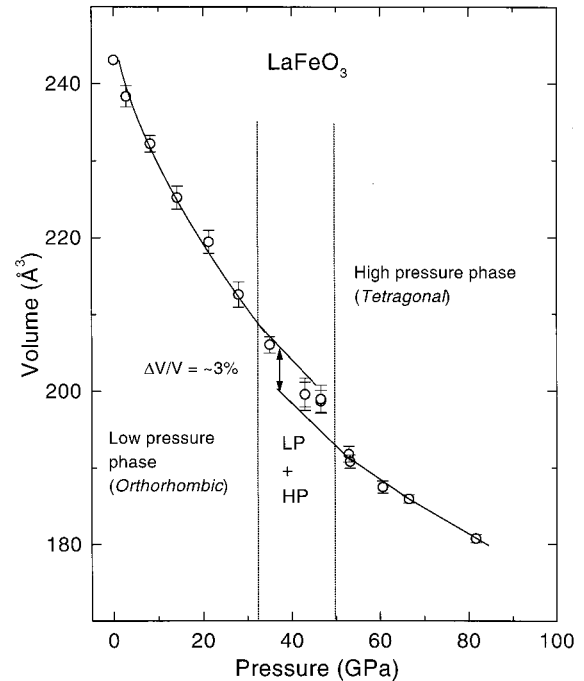


FIG. 1. Pressure dependence of the volume in LaFeO_3 using synchrotron XRD data collected in the angle dispersive mode. A sluggish transition to a tetragonal structure and a $\sim 3\%$ drop in volume take place in the 35- to 50-GPa range.

transition to the denser HP phase an abrupt decrease in IS [an increase in $\rho_s(0)$] is observed as can be seen in the lower inset of Fig. 3.

The first-order phase transition coincided with significant changes in both the magnetic and electronic properties as

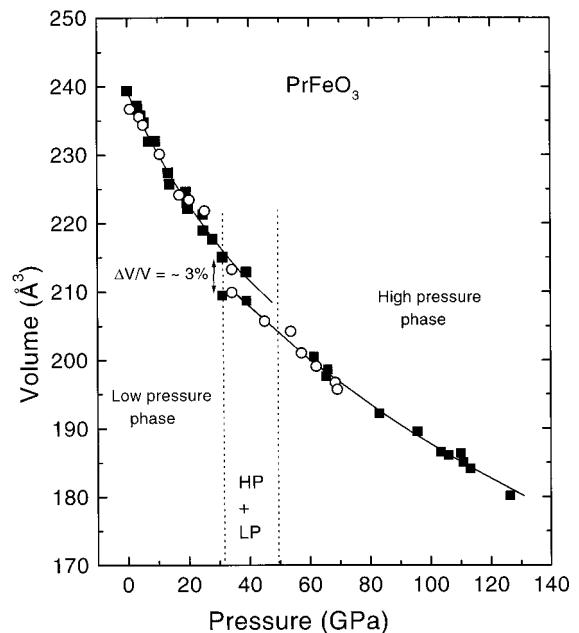


FIG. 2. Pressure dependence of the volume in PrFeO_3 using synchrotron XRD data collected both in energy (\circ) and angle dispersive (\blacksquare) modes. A $\sim 2.8\%$ drop in volume is observed in the 35- to 50-GPa range.

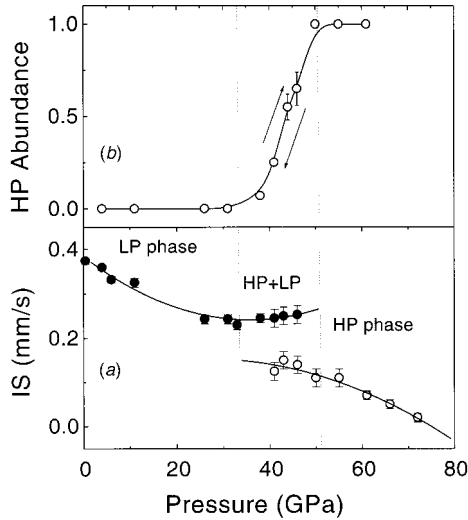


FIG. 3. (a) The $IS(P)$ dependence near the phase transition for PrFeO_3 is shown in (a). The abrupt drop in the IS near 35 GPa, corresponding to an abrupt increase in the electron density $\rho_S(0)$ at the nucleus, is consistent with the crystallography findings. The HP-phase values of the IS are the average of the values corresponding to the LS and HS states. (b) The pressure dependence of the relative abundance of the HP phase as deduced from the MS absorption area of PrFeO_3 . The curve implies that there is no significant pressure hysteresis. The solid lines are to guide the eyes.

demonstrated by the MS and resistance findings. A typical example of the evolution in the Mössbauer spectra with pressure is shown in Fig. 4 for PrFeO_3 . At ambient temperature, starting at ~ 35 GPa, one observes a sluggish transition from the LP antiferromagnetic state into a HP nonmagnetic phase. In the pure LP phase, extending from 0–35 GPa, the deduced H_{hf} at 300 K is 51 T, typical of a Fe^{3+} high-spin ($3d^5$, ${}^6A_{1g}$) configuration; H_{hf} increases slightly with pressure due to an increase in the Néel temperature (T_N). Also, above 35 GPa one notices a magnetic component characterized by a somewhat smaller hyperfine field (H_{hf}) of ~ 48 T at RT, but a similar IS value. The fact that its IS is similar to that of the LP phase suggests that this component still belongs to the original phase probably reflecting a slight distortion in the Fe-O bonding.

Careful inspection of the HP nonmagnetic phase reveals two quadrupole-split (QS) components with equal abundance. The presence of these two components is even more convincingly visualized by cooling the sample (at 43 GPa) to 100 K where the QS value of one of HP component increases (see Fig. 5). Full conversion to a nonmagnetic state at 300 K is attained by ~ 50 GPa. By following the relative HP phase abundance, based on the relative areas associated with the MS components, one finds no significant pressure hysteresis associated with this structural transformation (see upper inset of Fig. 3).

The effects of pressure on the electrical resistance $R(P)$ for LaFeO_3 and PrFeO_3 at room temperature are shown in the main body of Figs. 6 and 7, respectively. The first discernible data were obtained at ~ 20 GPa. With increasing pressure, particularly in the LP+HP coexistence pressure

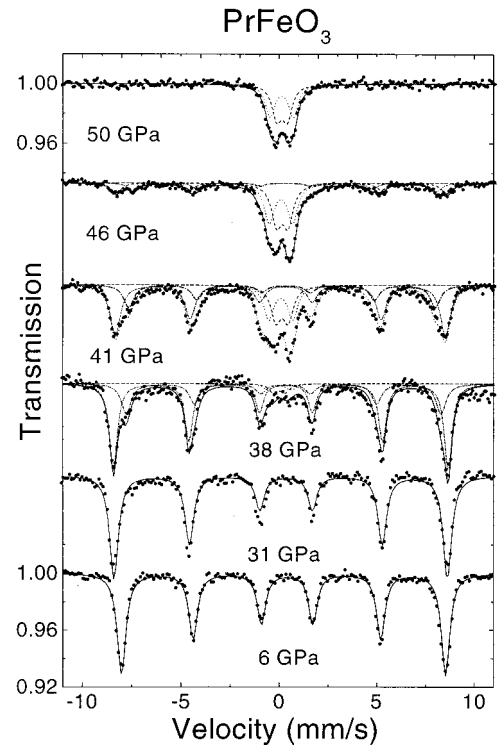


FIG. 4. Mössbauer spectra of PrFeO_3 below 50 GPa at RT. Similar spectra but of lower quality were observed with LaFeO_3 (see Ref. 13). The smooth lines are theoretical spectra deduced from least-squares fits to the experimental data. At 6 and 31 GPa, the spectra correspond to a pure LP phase consisting of a single magnetic component typical of a HS Fe^{3+} . By 38 GPa, a pressure in the coexistence regime, one observes a partial transformation of the ferric HS component into a second magnetic component with a smaller H_{hf} , whose origin is not known, and a nonmagnetic phase corresponding to the HP phase and characterized by two quadrupole-split components. At 46 GPa very little is left of the LP-phase component and at 50 GPa, within the pure HP phase, the only components observed are the two nonmagnetic ones.

range, a precipitous drop in $R(P)$ is observed indicative of the onset of gap closure at higher pressure. The inset figures are discussed later.

B. The high-pressure phase

1. Mössbauer results

At $T > 100$ K the HP phase at its inception (> 35 GPa) is composed of two equiabundant Fe^{3+} nonmagnetic components, each characterized by its own values of QS and IS. The nature of these two components becomes evident upon cooling below 100 K. At low temperatures (see Figs. 8 and 9) the component with the *smaller* quadrupole splitting (QS ~ 1.2 mm/s, IS ~ 0.134 mm/s) splits magnetically into a well-defined sextet with $H_{\text{hf}} = 47$ T, a value within the range of high-spin ($S = \frac{5}{2}$, ${}^6A_{1g}$) ferric ions. The component with the *larger* QS (QS ~ 2.40 mm/s, IS ~ 0.07 mm/s) shows a broad, unresolved magnetic-split spectrum. Thus the ordered state is composed of two magnetic sublattices. Another consequence of the volume contraction is the considerable drop

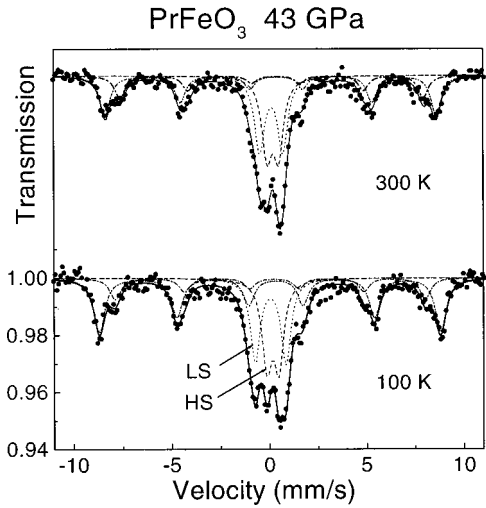


FIG. 5. Mössbauer spectra of PrFeO_3 recorded in the coexistence region (43 GPa) at 296 and 100 K. The strong QS temperature dependence of the component with the larger QS substantiates its LS assignment (see text).

of the magnetic ordering temperature, from well above 700 K in the LP phase to ~ 100 K.¹⁴ As will be shown, the origin of the broad spectral component is the onset of a magnetic spin relaxation of the low-spin (LS) Fe^{3+} state ($S = \frac{1}{2}$, $^2T_{2g}$). With further pressure increases a spin crossover of the high-spin (HS) component is clearly observed; at 61 GPa (Figs. 8 and 9), the dominating phase is the LS ferric iron. At ~ 70 GPa the HS sublattice is completely transformed into the LS state.

The spin Hamiltonian governing the hyperfine interaction of the magnetic split, perturbed by a small electric-quadrupole interaction of the $\frac{1}{2} \leftrightarrow \frac{3}{2}$ transition in ^{57}Fe can be described as

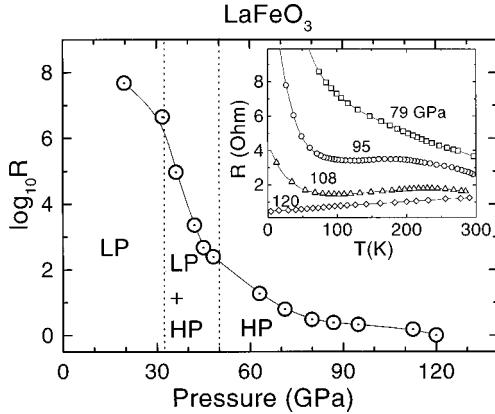


FIG. 6. The pressure dependence of the resistance of LaFeO_3 at 300 K. In the coexistence range a precipitous reduction in the resistance is found, coinciding with the first-order volume reduction. The resistance levels off at $P > 90$ GPa. Typical $R(T)$ dependencies for $P > 79$ GPa are shown in the inset. The temperature onset of the metallic state ($dR/dT > 0$) is evident in the 95- to 108-GPa range, culminating into a fully metallic state for $P > 120$ GPa. A curve fit to $R(T)$ at 120 GPa and below 100 K shows a T^2 dependence, expected for a correlated metal (metal with moments).

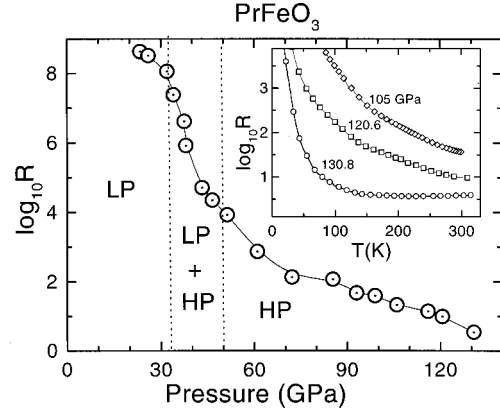


FIG. 7. The pressure dependence of the resistance of PrFeO_3 at 300 K. In the coexistence regime a precipitous decrease in the resistance is clearly seen, coinciding with first-order volume reduction. Relative to the ~ 20 -GPa value the resistance drop is smaller than that in LaFeO_3 , because of its higher compressibility. Whereas LaFeO_3 is completely metallized for $P > 110$ GPa, PrFeO_3 shows pure metallic behavior only at $T > 110$ K [see $R(T)$ curve inset] and at P above ~ 131 GPa.

$$H = \mu H_{\text{hf}}(I_z/I) + \{e^2 q_{zz} Q(3 \cos^2 \theta - 1)/[8I(2I - 1)]\} \times \{3I_z^2 - I(I - 1)\}, \quad (1)$$

where $e^2 q_{zz} Q$ is the quadrupole coupling constant ($= 2 \times \text{QS}$), and θ is the angle formed between the magnetic moment μ and the electric-field-gradient principal axis q_{zz} .

The theoretical fit to the magnetic relaxation spectra was carried out using the formalism developed for ^{166}Er MS in ErFeO_3 by Nowik and Wickman.¹⁵ This relatively simple formalism assumes two spin state manifolds, e.g., the spin up (ω_A) and spin down (ω_B) characterized by $(S = \frac{1}{2}, I = \frac{1}{2}) \rightarrow (S = \frac{1}{2}, I = \frac{3}{2})$ and $(S = -\frac{1}{2}, I = \frac{1}{2}) \rightarrow (S = -\frac{1}{2}, I = \frac{3}{2})$ transitions, respectively. The two $S = \pm \frac{1}{2}$ are separated by a distinctive energy Δ (see Fig. 10). The intensity I_{AB} of the Mössbauer spectra describing the transition mechanism is given by

$$I_{AB}(\omega) = K \frac{(1 + \tau\Gamma)P + QR}{P^2 + R^2} \quad (2)$$

with

$$P = \tau[\Gamma^2 - (\omega_0 - \omega)^2 + \delta^2] + \Gamma,$$

$$R = (\omega_0 - \omega)(1 + 2\tau\Gamma) + (p_B - p_A)\delta,$$

$$Q = \tau[\omega_0 - \omega - (p_B - p_A)\delta], \quad \omega_0 = \frac{1}{2}(\omega_B + \omega_A),$$

$$\delta = \frac{1}{2}(\omega_B - \omega_A).$$

The states will exchange energy ($\omega_B \leftrightarrow \omega_A$) within a typical relaxation time τ . The relative probabilities of the system to be in states ω_B and ω_A are given by p_B and p_A , where ($p_B + p_A = 1$) and $p_A/p_B = f(\Delta)$.¹⁶ We characterize the para-

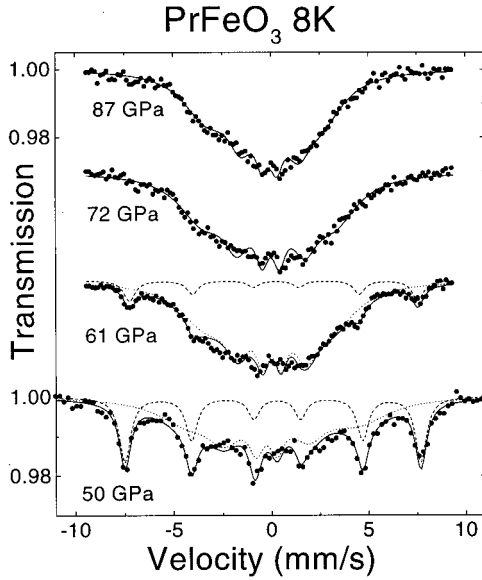


FIG. 8. The HP-phase, low-temperature Mössbauer spectra of PrFeO_3 . At 50 GPa, just above the coexistence region, the two QS components (see Fig. 4) split magnetically into HS and LS components. The first is characterized by a static magnetic hyperfine interaction $H_{\text{hf}}=45$ T and the second by a spin-spin magnetic relaxation spectrum. With increasing pressure, a gradual spin-crossover occurs, culminating in a pure LS state at $P>70$ GPa. At 50–61 GPa the dotted lines are a theoretical fit to the magnetic relaxation spectra using expressions (1) and (2) and the dashed lines are a theoretical fit to a static spin Hamiltonian using expression (1). The fitting of spectra at $P>70$ GPa assumes the presence of a single LS component.

magnetic relaxation regime as that where $p_B=p_A=0.5$, and therefore $\Delta=0$. In the magnetic relaxation regime $p_B \neq p_A$ and $\Delta \neq 0$.¹⁷ The least-squares fits to the experimental Mössbauer spectra were carried out by constraining the values of IS and Γ to those deduced in the paramagnetic state at a low temperature close to T_N . Due to limitations imposed by the poor spectral resolution, p_B and τ are strongly statistically correlated. Following trial and error tests, the best fits of the magnetic relaxation spectra were obtained by fixing τ to 8×10^{-9} s and allowing p_B to vary as a function of pressure. Attempts to fix p_B and vary τ resulted in poor fits. Spectra of PrFeO_3 at 8 K and LaFeO_3 at 5 K (far below the ordering temperatures) in the 50-to 170-GPa range (the HP phase) are shown in Figs. 8 and 9, respectively. In Fig. 11 we show the pressure dependence of p_B as deduced from the least-squares fit. We see that p_B increases monotonically with pressure, indicating a decrease in Δ towards zero when p_B reaches 0.5 at higher pressures. The temperature dependence of the spectra of the PrFeO_3 measured at 72 GPa ($S=\frac{1}{2}$) is shown in Fig. 12. In the fitting process the only variables were p , τ , QS, and H_{hf} . As can be seen the theoretical fit of the data is excellent. It was found that p and τ are practically temperature independent, e.g., mediation by phonons is minimal, suggesting that the magnetic relaxation process is due to pure spin-spin interaction. From the uppermost $H_{\text{hf}}(T)$ graph we obtain by extrapolation the ordering temperature at 72 GPa to be ~ 110 K.

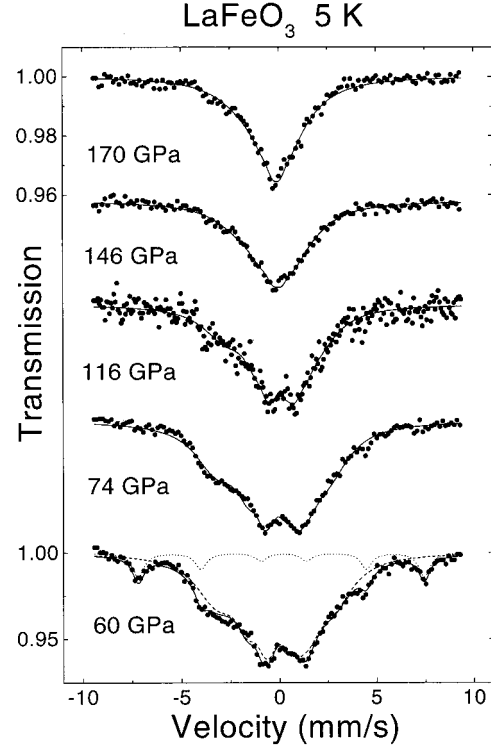


FIG. 9. The low-temperature Mössbauer spectra of the HP phase of LaFeO_3 at $P>60$ GPa. Both the HS and LS components are observed at 60 GPa. The fitting procedure was similar to that in PrFeO_3 (Fig. 8). At ~ 120 GPa a change in the spin interactions takes place involving a spin-lattice paramagnetic relaxation mechanism. Spectra at $P>120$ GPa were fitted with expressions (1) and (2) by fixing p_B to 0.5 (see text).

In LaFeO_3 at >120 GPa we reach the regime of paramagnetic relaxation. This is evident in Fig. 9. The spectrum at 116 GPa is quite symmetrical and that at and above 146 GPa is typical of paramagnetic relaxation spectra observed in ^{57}Fe MS.¹⁹ Expressions (1) and (2) were used for the fit procedures but with p_B fixed to 0.5. Again this theoretical fit is quite reasonable. At low temperatures as the pressure is increased, the spectra narrow due to a decrease of H_{hf} . The temperature dependence of the Mössbauer paramagnetic relaxation spectra for LaFeO_3 at 170 GPa is shown in Fig. 13. Parameters were fixed except for the relaxation time τ and H_{hf} which was determined to vary from $\sim 5 \times 10^{-8}$ s at 8 K to 1×10^{-12} s at 300 K. At high temperatures $\tau \ll 10^{-7}$ s (the lifetime of the ^{57}Fe Mössbauer level), and a pure quadrupole-split spectrum is observed. The fact that τ is strongly temperature dependent implies a mechanism of spin-lattice relaxation, a process mediated by phonons in contrast to the spin-spin magnetic relaxation mechanism obtained at lower pressures.

2. Electrical resistance

The pressure dependencies of the resistance of LaFeO_3 and PrFeO_3 measured at 300 K are shown in Figs. 6 and 7. Following the precipitous decrease in R within the LP+HP coexistence range, a steady albeit sluggish decrease in $R(P)$

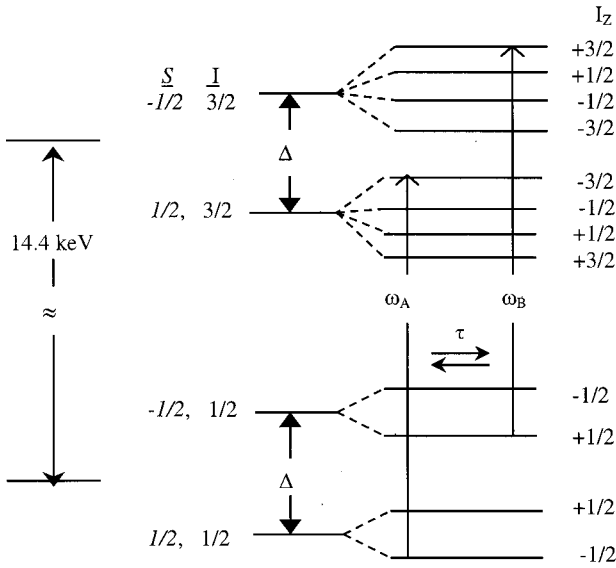


FIG. 10. The two spin states manifold with spin-up ω_A ($S = +\frac{1}{2}$) and spin-down ω_B ($S = -\frac{1}{2}$) configurations. The Mössbauer hyperfine transitions are between the nuclear Zeeman-split excited ($I = \frac{3}{2}$) and ground ($I = \frac{1}{2}$) states. The two S states are separated by a distinctive energy Δ of the order of $k_B T$ and exchange energy with a characteristic time τ . As long as $p_A = p_B$ a magnetic relaxation process is present and a finite magnetic ordering is present below a certain temperature. With increasing pressures and once $p_A = p_B$ a paramagnetic relaxation will be found.

is observed, perhaps a prelude to metallization. Indeed, $R(T, P)$ measurements performed in the HP phase (see insets of Figs. 6 and 7) clearly substantiate that metallization has occurred at the high pressures. In LaFeO_3 at >120 GPa, metallization ($dR/dT > 0$) is present at all temperatures. At lower pressures above ~ 95 GPa, metallization appears above some onset temperature. In PrFeO_3 at 131 GPa, the highest pressure reached in this study, clear indication of metallization is observed only above an onset temperature of ~ 150 K. The need for higher pressures is related to the relatively low compressibility of the HP phase of PrFeO_3 (see Figs. 1 and 2). This is shown by plotting $\log_{10} R$ as a function of the volume contraction. The volume contraction dependence of the resistance for the HP phase is shown in Fig. 14. We find

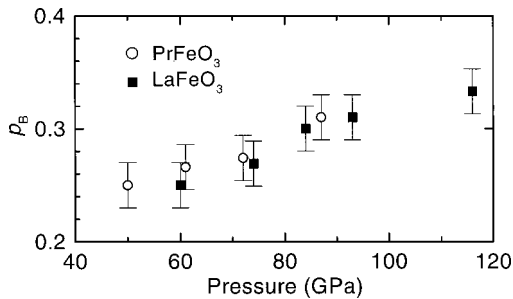


FIG. 11. The pressure dependence of the relative probability p_B of the system to be in the $S = +\frac{1}{2}$ state for $R\text{FeO}_3$. With pressure, p_B approaches the asymptotic value of 0.5 and the system becomes paramagnetic and a paramagnetic relaxation process is possible.

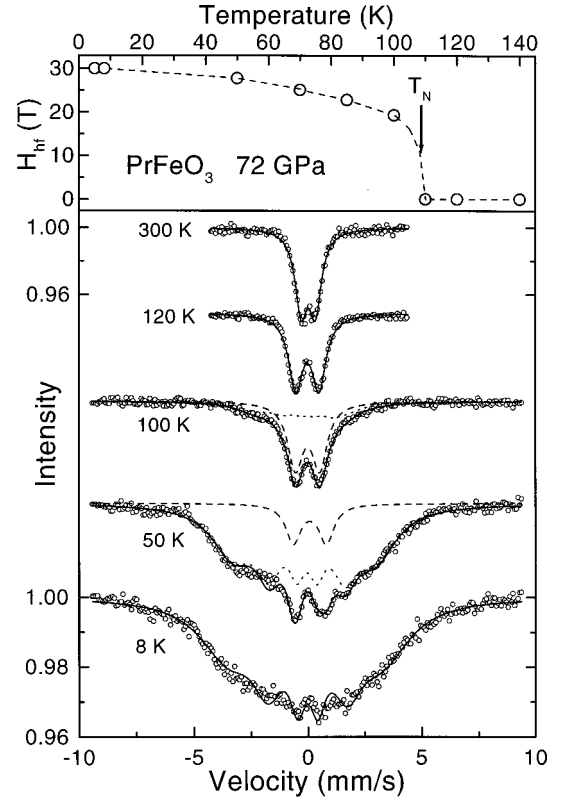


FIG. 12. The temperature dependence of the PrFeO_3 Mössbauer hyperfine spectra at 72 GPa within the LS magnetic relaxation regime. The fits utilize expressions (1) and (2) (see text). H_{hf} was the only variable parameter for $T < 100$ K H_{hf} is proportional to the magnetization. H_{hf} decreases with temperature and is null at ~ 110 K, the ordering temperature, as is shown in the upper part of the figure. A strong temperature dependence of the size of QS is evident in the paramagnetic spectra at 120 and 300 K.

that the $\log_{10} R$ results scale very well with volume contraction. Full metallization of PrFeO_3 at ~ 175 GPa is implied.

IV. DISCUSSION

From our analysis of the MS and resistance results in the HP regime, it is shown that the onset of metallization and the paramagnetic relaxation occur at $\Delta V/V_0 > 0.30$. For LaFeO_3 this occurs at $P \geq 120$ GPa, and for PrFeO_3 $P > 170$ GPa is estimated. As will be shown these two phenomena are strongly associated.

The phenomenon of a second-order pressure-induced HS \rightarrow LS transition is not surprising; it follows the progressive collapse of Hund's rule concerning the energetically favorable HS state.¹⁸ A similar pressure-induced, second-order spin crossover has been observed in Fe^{2+} in FeO (Ref. 19) and FeS .²⁰ Upon the completion of the spin crossover in Fe^{3+} , the process of metallization starts. This is accompanied or caused by a drastic deterioration of the exchange and superexchange interactions between the LS ferric ions. As long as $p_B < 0.5$ an interaction between moments is present mediated by a finite (molecular) exchange field. The hyperfine field H_{hf} in a Fe^{3+} LS state is composed of two main terms,

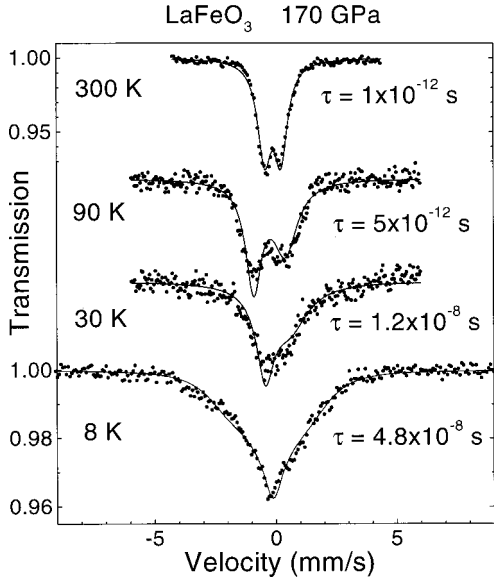


FIG. 13. The temperature dependence of the Mössbauer hyperfine spectra of LS LaFeO₃ at 170 GPa within the paramagnetic relaxation regime. As shown, the relaxation time τ decreases rapidly with increasing temperature, an indication of a spin-lattice relaxation process.

namely, $H_{\text{hf}} = H_F + H_L$ where H_F is the Fermi contact term, which is proportional to the spin density at the nucleus [$H_F \propto \langle \Psi^\uparrow(0)^2 - \Psi^\downarrow(0)^2 \rangle$], which is proportional to the moment $\langle S_z \rangle$, and where H_L is the orbital moment term expressed as $H_L \propto \langle r^{-3} \rangle (g-2) \langle S_z \rangle$ where $\langle r^{-3} \rangle$ is the average radius of the valence d electrons. Thus, we may express the total hyperfine field as

$$H_{\text{hf}} \propto \langle S_z \rangle [\text{ct} + \text{orb} \langle r^{-3} \rangle], \quad (3)$$

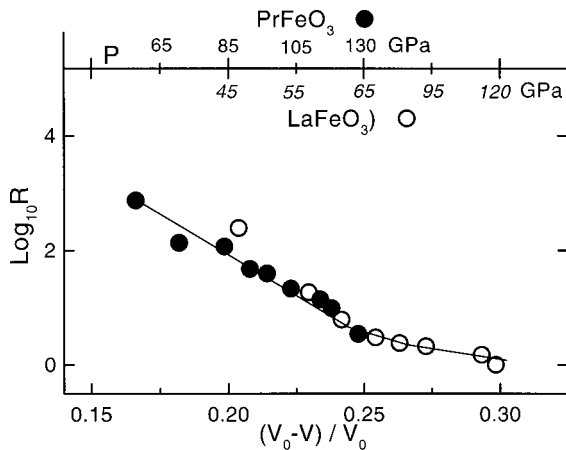


FIG. 14. The variation of the resistance of LaFeO₃ and PrFeO₃ in the HP phase as a function of the relative volume contraction. The $[V_0 - V(P)]/V_0$ volume scale reflects the difference in the equation of states of both materials (see Figs. 1 and 2). V_0 is the volume at ambient pressure. The curve serves as a guide to the eye. From this plot one predicts the onset of a metallic (and paramagnetic) state of the less compressible PrFeO₃ at ~ 175 GPa (see text).

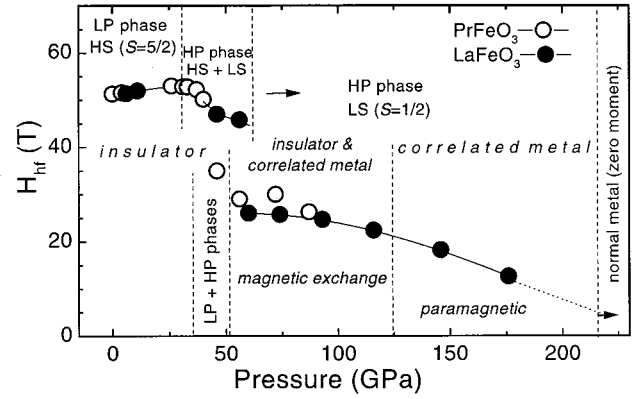


FIG. 15. The phase diagram of $R\text{FeO}_3$ in terms of the hyperfine field as a function of pressure (see text). The solid lines are guides to the eye, and the vertical dotted lines delineate various ranges in the Mott-Hubbard diagram. In the LP phase, up to ~ 35 GPa, H_{hf} increases slightly possibly due to the increase in T_N with P . In the 35- to 50-GPa pressure range the HP and the LP phases coexist, and between 50–70 GPa the HP phase is composed of both LS and HS states with the abundance of the HS decreasing with pressure. Up to ~ 70 GPa the material is a bona fide insulator ($U/t > 1$). Beginning at 70 GPa, up to 120 GPa, the LS state still shows magnetic exchange with a progressive decrease of the H_{hf} (magnetic moment). In this range both the correlated metal and the insulator states coexist with the abundance of the latter decreasing with increasing pressure. The state at $P > 120$ GPa is paramagnetic, and the metal is correlated. In LaFeO₃, based on extrapolation to $H_{\text{hf}} = 0$, a normal-metal state ($U/t \ll 1$) is expected to occur at ~ 220 GPa.

where “ct” stands for the Fermi contact term constant, which for the LS Fe³⁺ is $-22 \langle S_z \rangle T$ or about -11 T, and “orb” is the orbital moment term constant. The fact that H_{hf} at the “inception” of the LS state, at 35 GPa, is ~ 25 T implies an orbital term of either -14 or $+36$ T since we do not determine the sign of H_{hf} .

Despite the spin fluctuations an effective magnetic ordering takes place, as shown in Fig. 12, characterized by an effective moment and ordering temperature. As can be seen the ordering temperature of the spin-magnetic fluctuating PrFeO₃ at 72 GPa is quite close to 110 K, and it decreases with increasing pressure.

Eventually at a higher pressure, once $p_B = p_A = 0.5$ and consequently $\Delta = 0$, the paramagnetic relaxation regime is established. The sheer presence of spin-spin magnetic relaxation phenomena at such high pressures and low temperatures is a manifestation of the frailty of the Fe³⁺ low-spin $S = 1/2$ moments and their corresponding interactions. The transition to a paramagnetic relaxation signals a completely disordered magnetic state, a system with noninteracting moments. This is, to the best of our knowledge, the first report of a pressure-induced magnetic or paramagnetic relaxation phenomenon. The onset of a paramagnetic regime is concurrent with full metallization. A fit of $R(T)$ for LaFeO₃ at 120 GPa shows a T^2 dependence to 100 K, consistent with the temperature behavior of a metal with moments.

As mentioned, the two extremes of a Mott-Hubbard system are $U \gg t$ and $U \ll t$. The first extreme (the correlated

system) is characterized by a large electronic gap and magnetic moments, and the second extreme represents an uncorrelated system where the material is a normal metal with no significant localized moments. In Fig. 15 we summarize the Mott-Hubbard phase diagram of the $R\text{FeO}_3$ system in the form of H_{hf} versus pressure. Whereas the hyperfine field, which is proportional to the magnetic moment, is taken as a measure of the correlation strength, the pressure coordinate represents t/U .

As seen in Fig. 15, the system is highly correlated with increasing pressures up to ~ 30 GPa, with a large optical gap and moment, the latter typical of an $S = \frac{5}{2}$ state. In the structural phase-transition pressure zone (the coexistence pressure range), the single magnetic state branches into two magnetic sublattices composed of HS and LS moments accompanied by a significant reduction of the gap. For LaFeO_3 in the 65- to 125-GPa range and for PrFeO_3 in the 65- to (probably) 175-GPa range we observe a pure LS state with weakly interacting moments, as evidenced by the presence of magnetic relaxation in the Mössbauer spectra. Here the $R(P, T)$ behavior indicates that the system is either in a mixed insulator-metal regime or on the verge of an insulator-metal transition. However, once the pressure exceeds 125 GPa for the case of LaFeO_3 (and perhaps 175 GPa for the case of PrFeO_3), the paramagnetic relaxation spectra show that the moments cease to interact. The presence of a correlated metal in LaFeO_3 is further substantiated by the $R(T)$ behavior at 120 GPa (inset of Fig. 6) where a $R = \alpha T^2$ dependence was found.

Following the first-order phase transition at ~ 35 GPa we find a gradual decrease of H_{hf} (or the magnetic moment) with pressure (or t/U) as is expected from the basic features of the Mott-Hubbard model. As can be seen from Eq. (3) and de-

spite the expected increase in $\langle r^{-3} \rangle$ with pressure, a continuous decrease in H_{hf} with pressure is observed, a manifestation of an accelerated breakdown of the correlated state.

At 170 GPa the hyperfine field (the LS moment) has decreased to less than half of its initial value at ~ 50 GPa. By extrapolating to $H_{\text{hf}}=0$ we conclude that it will take $P > 200$ GPa to achieve a correlation breakdown where LaFeO_3 will become a normal metal.²¹

V. CONCLUSION

By combining the powerful methods of synchrotron XRD, resistance, and Mössbauer spectroscopy to 170 GPa a detailed study of the progressive breakdown of a correlated system, the LaFeO_3 and PrFeO_3 rare-earth orthoferites, could be followed. The 3% volume contraction at 30 GPa initiates the collapse of the strong correlation and the creation of two magnetic sublattices, reflecting a HS and a LS Fe^{3+} presence. At ~ 60 GPa a complete spin crossover takes place in both compounds. For LaFeO_3 , in the 120- to 170-GPa range a metal with moments phase is established coinciding with the onset of a paramagnetic relaxation regime in which the further reduced and ineffective moments no longer interact. By extrapolation, a normal metal is expected at ~ 220 GPa. The same basic phenomena are predicted for PrFeO_3 , but at higher pressures.

ACKNOWLEDGMENTS

This research was supported in part by a LANL-UC IGPP program Grant No. 919R, by BSF Grant No. 9800003, and by the Israeli Science Foundation Grant No. 1998003. We thank the personnel of the ID30 beam (ESRF) and that of the HP beam (CHESS) for their assistance.

¹N. F. Mott, *Metal-Insulator Transitions* (Taylor & Francis, London, 1990), and references therein.

²An exceptional case of a temperature-dependent Mott transition has been observed in $R\text{NiO}_3$ [see J. B. Torrance *et al.*, Phys. Rev. B **45**, 8209 (1992)].

³The Hubbard Hamiltonian $H = \sum t_{ij} a_{i\sigma}^\dagger a_{j\sigma} + U \sum n_i^\uparrow n_i^\downarrow$ is the simplest description of a Mott insulator [J. Hubbard, Proc. R. Soc. London, Ser. A **277**, 237 (1964)]. It is characterized by a kinetic-energy term t_{ij} denoting the hopping of an electron from site i to its nearest-neighbor site j and by the extra energy cost U of putting two electrons ($n_i^\uparrow n_i^\downarrow$) on the same site. The bandwidth W is proportional to t . In the case of a charge-transfer insulator U , the energy gap separating the empty and filled d bands is replaced by Δ , a gap between the empty d band, and filled-ligand bands [J. G. Zaanen, G. A. Sawatzky, and J. W. Allen, Phys. Rev. Lett. **55**, 418 (1985)].

⁴S. A. Carter, T. F. Rosenbaum, M. Lu, H. M. Jaeger, P. Metcalf, J. M. Honig, and J. Spalek, Phys. Rev. B **49**, 7898 (1994).

⁵M. P. Pasternak, R. D. Taylor, A. Chen, C. Meade, L. M. Falicov, A. Giesekus, R. Jeanloz, and P. Y. Yu, Phys. Rev. Lett. **65**, 790 (1990).

⁶M. P. Pasternak, R. D. Taylor, and R. Jeanloz, *Frontiers of High*

Pressure Research, edited by H. D. Hochheimer and R. D. Eters (Plenum, New York, 1992), p. 227.

⁷M. P. Pasternak, G. Kh. Rozenberg, G. Yu. Machavariani, O. Naaman, R. D. Taylor, and R. Jeanloz, Phys. Rev. Lett. **82**, 4663 (1999).

⁸G. Yu. Machavariani, M. P. Pasternak, G. R. Hearne, and G. Kh. Rozenberg, Rev. Sci. Instrum. **69**, 1423 (1998).

⁹Due to the proximity of electrodes ($\sim 10 \mu\text{m}$), there was no need for a pressure medium.

¹⁰A. P. Hammersley, S. O. Svensson, M. Hanfland, A. N. Fitch, and D. Hausermann, High Press. Res. **14**, 235 (1996).

¹¹Obtained from the Max Planck Institute for Solid State, Stuttgart, Germany.

¹²G. R. Hearne, M. P. Pasternak, and R. D. Taylor, Rev. Sci. Instrum. **65**, 3787 (1994).

¹³G. R. Hearne, M. P. Pasternak, R. D. Taylor, and P. Lacorre, Phys. Rev. B **51**, 11 495 (1995).

¹⁴The T_N for each pressure was deduced from $H_{\text{hf}}(T, P)$ measurements and extrapolation to $H_{\text{hf}}=0$.

¹⁵I. Nowik and H. H. Wickman, Phys. Rev. Lett. **17**, 949 (1966).

¹⁶Nowik and Wickman (Ref. 15) assume $F(\Delta) = \exp(\Delta/kT)$. However in the present (P, T) range we find $F(\Delta)$ is pressure depen-

- dent but temperature independent to a first approximation.
- ¹⁷F. Van der Woude and A. J. Dekker, *Phys. Status Solidi* **9**, 775 (1965).
- ¹⁸D. M. Sherman, in *Advances in Physical Geochemistry*, edited by S. K. Saxena (Springer-Verlag, Berlin, 1988), Vol. 7, p. 113.
- ¹⁹M. P. Pasternak, R. D. Taylor, R. Jeanloz, X. Li, J. H. Nguyen, and C. A. McCammon, *Phys. Rev. Lett.* **79**, 5046 (1997).
- ²⁰H. Kobayashi, M. Sato, T. Kamimura, M. Sakai, H. Onodera, N. Kuroda, and Y. Yamaguchi, *J. Phys.: Condens. Matter* **9**, 515 (1997).
- ²¹For PrFeO₃ at an extrapolated pressure of 240 GPa the material will become a normal metal.